*Mathematical Medicine and Biology* (2013) **30**, 1–19
doi:10.1093/imammb/dqr023
Advance Access publication on October 17, 2011

# Are more complicated tumour control probability models better?

JIAFEN GONG, MAIRON M. DOS SANTOS, CHRIS FINLAY AND THOMAS HILLEN*
*Centre for Mathematical Biology, Department of Mathematical & Statistical Sciences, University of Alberta, Edmonton, AB T6G 2G1, Canada*
*Corresponding author: thillen@ualberta.ca

[Received on 2 December 2010; revised on 29 June 2011; accepted on 12 August 2011]

Mathematical models for the tumour control probability (TCP) are used to estimate the expected success of radiation treatment protocols of cancer. There are several TCP models in the literature, from the simplest (Poissonian TCP) to the well-advanced stochastic birth–death processes. Simple and complex models often make the same predictions. Hence, here, we present a systematic study where we compare six of these TCP models: the Poisson TCP, the Zaider–Minerbo TCP, a Monte Carlo TCP and their corresponding cell cycle (two-compartment) models. Several clinical non-uniform treatment protocols for prostate cancer are employed to evaluate these models. These include fractionated external beam radiotherapies, and high and low dose rate brachytherapies. We find that in realistic treatment scenarios, all one-compartment models and all two-compartment models give basically the same results. A difference occurs between one-compartment and two-compartment models due to reduced radiosensitivity of quiescent cells. We find that care must be taken for the right choice of parameters, such as the radiosensitivities $\alpha$ and $\beta$ and the hazard function $h$. Typically, different hazard functions are used for fractionated treatment (fractionated survival fraction) and for brachytherapies (Lea−Catcheside protraction factor). We were able to combine these two approaches into one 'effective' hazard function. Based on our results, we can recommend the use of the Poissonian TCP for everyday treatment planning. More complicated models should only be used when absolutely necessary.

*Keywords*: tumour control probability; radiation treatment of cancer; mathematical modelling of cancer treatment.

## 1. Background

A standard treatment for the control of tumour growth is radiation. Many mathematical models have been developed to help predict the outcome of a given radiation treatment schedule. One such mathematical tool is the tumour control probability (TCP). The TCP is a measure for the probability of tumour cell eradication and it can be used to compare the expected success of different treatment protocols. The very nature of tumour control, i.e. the eradication of clonogenic cells, requires a stochastic approach for the TCP. There are several TCP models in the literature, which are based on Poisson statistics, on general birth–death processes, on branching processes, and on individual-based models. Several of these models have been validated using clinical data (Stavreva *et al.*, 2003; Horas *et al.*, 2010); hence, we are confident about the significance of these models. While the first models are based on a single clonogenic population (Zaider & Minerbo, 2000; Hanin, 2001), extensions have been presented which aim to include cell cycle or quiescent states (Dawson & Hillen, 2006; Hillen *et al.*, 2010; Maler & Lutscher, 2010). Some of these models are fairly simple (e.g. the Poissonian TCP), while others are very complex (e.g. a TCP model from a cell cycle birth–death process). In practice, it is hard to judge which of these

models should be used. What do we loose if we still use the simple model and not the more complicated alternatives?

The purpose of this paper is to show that, in realistic treatment scenarios for prostate cancer, all models give very similar results. Discrepancies can be observed, although they are small compared to other uncertainties that are intrinsic in these models. Our conclusion is that the Poissonian TCP model is good enough for everyday treatment planning, in particular when it comes to the comparison of different treatment protocols. More complicated models should only be used if there is a striking reason to do so. This confirms the theoretical results obtained by Hanin (2004), who showed that in the limit for large tumours and not too fast growing tumours, the distribution of surviving tumour cells approximates a Poisson (or generalized Poissonian) distribution.

Some work has been done on the comparison of different TCP models: Tucker *et al.* (1990) first questioned the efficacy of the Poissonian TCP by numerical simulation and found that the Poissonian TCP might underestimate the correct TCP. In an example of a very fast growing tumour, the discrepancy was about 15%. Yakovlev (1993) confirmed these findings theoretically, and Hanin and his group (Hanin, 2001, 2004; Hanin *et al.*, 2001) proved, mathematically, that the TCP based on the iterative birth–death process converges to a Poissonian TCP for uniform fractionated treatment.

The six TCP models compared in this paper are as follows:

(1-P): **The Poissonian TCP.** The Poissonian TCP is the standard formula for TCP computations for uniform fractionated treatments. There are several extensions of this model which include regrowth or lesion repair mechanisms, and we will discuss those later in Section 2.

(1-ZM): **The TCP of Zaider & Minerbo (2000).** The TCP of Zaider and Minerbo is based on a birth–death process for tumour growth and decay. It is the first model which allows for arbitrary temporal form of radiation treatment and the approach of Zaider and Minerbo has revolutionized the field.

(1-MC): **Monte Carlo TCP.** Here we explicitly simulate a large number of cells and use Monte Carlo simulations to estimate tumour survival.

(2-P): **Two-compartment Poissonian TCP.** Here we aim to include cell cycle mechanisms. We split the cell populations into two compartments which represent an active phase (G1, S, G2, M) and a quiescent phase (G0). If the clonogenic cells do not enter a G0 phase, then the model equally applies for a splitting into S, G2, M and G1 phases. The major assumption is that active cells are more radiosensitive compared to cells in the quiescent compartment.

(2-DH): **Two-compartment TCP of Dawson & Hillen (2006).** The Dawson and Hillen TCP is based on a birth–death process and generalizes the ZM TCP, aiming to include cell cycle effects according to the splitting mentioned in item (2-P).

(2-MC): **Two-compartment Monte Carlo TCP.** Here we extend the Monte Carlo simulations to the two-compartment scenario.

These models depend on a number of parameters, e.g. the initial number of tumour cells $n_0$, the radiation sensitivities $\alpha$ and $\beta$, or the so-called 'hazard function' $h(t)$. We will test several combinations of the parameter values and we give details about the models and parameters in Sections 2 and 3. In Section 4, we present our results and we conclude the paper with a discussion in Section 5.

### 1.1 *Prostate cancer*

Prostate cancer is the most common malignant tumour afflicting men in the world (World Health Organization, 2008). Fortunately, early detection tests—such as digital rectal examination or determining the amount of prostate-specific antigen (PSA) in the blood—increase the chance of early diagnosis and hence successful treatment (American Cancer Society). One very important treatment method for prostate cancer is radiotherapy, where ionizing particles (such as X-rays and gamma-rays) transfer energy and kill cancer cells in the treated area. Over half of all cancer patients receive radiotherapy at some stage of their disease, either alone or in combination with other types of treatment (such as surgery or chemotherapy) (Kaanders *et al.*, 2002; O'Rourke *et al.*, 2009). Two types of radiotherapy methods are available: brachytherapy, whereby a radiation probe is inserted into the tumour; and external beam radiotherapy, in which the tumour is irradiated from outside the patient. Generally speaking, in external beam radiotherapy, the total dose (energy per unit mass in unit of gray (Gy)) is split into several fractions to allow the patient's normal tissues to recover between fractions.

Brachytherapy is more efficient for early stage, localized prostate cancer. There are two brachytherapy methods for prostate cancer: high dose rate and permanent seeds (also called low dose rate) brachytherapy (Prostate Cancer Canada). High dose rate brachytherapy involves inserting several fractions of seeds, over a span of a few days, through very tiny plastic catheters placed into the prostate gland. In low dose rate brachytherapy, seeds are injected into the glands. These seeds will irradiate off at a low dose rate and remain in the gland for a long time. If we denote the initial dose as $R_0$ and the seed decay rate as $\lambda$, then the total dose $D(t)$ absorbed up to time $t$ is given by

$$D(t) = \frac{R_0}{\lambda}(1 - \mathrm{e}^{-\lambda t}). \tag{1.1}$$

## 2. TCP models

Before we introduce the TCP models, we briefly discuss the linear quadratic (LQ) model for cell survival and the hazard function.

### 2.1 *Survival fraction*

If $D$ denotes the radiation dose, then we denote the survival fraction of cells as $S(D)$. A widely accepted survival fraction model is the LQ model:

$$S(D) = \exp(-\alpha D - \beta D^2), \tag{2.1}$$

where $\alpha$ $(Gy^{-1})$ and $\beta$ $(Gy^{-2})$ are radiosensitivity parameters depending on the tissue types. The parameters $\alpha$ and $\beta$ are empirically estimated parameter values and they include radiosensitivity as well as repair mechanisms. The ratio $\alpha/\beta$ is a rough characterization of the sensitivity of tissues to radiation and it can be used to differentiate tissues into early responding tissue ($\alpha/\beta \approx 10$, typical for clonogenic tissue) or late responding tissue (the ratio is about 3, typical for healthy tissue) (Wheldon, 1988; Fowler, 1989).

When the treatment dose $D$ is split into $n$ fractions of dose $d$, $D = nd$ and the survival for each fraction is independent, (2.1) changes into

$$S(D(n,d)) = \underbrace{\exp(-\alpha d - \beta d^2) \cdots \exp(-\alpha d - \beta d^2)}_{n} = \exp(-\alpha D - \beta d D) = \exp(-(\alpha + \beta d)D). \tag{2.2}$$

Equations (2.1) and (2.2) assume that there is no regrowth during treatment. However, proliferation plays an important role when the treatment time is long compared to the tumour doubling time. Travis & Tucker (1987) were the first to include a time factor in the LQ model. By fitting mouse lung cancer data of Mah *et al.* (1987), they found that the regrowth is exponential with parameter $b$ and the isoeffect curves $E$ ($= -\ln S(D)$) are constant,

$$E = \beta D(\alpha/\beta + D/n) - bT, \tag{2.3}$$

where $n$ is the number of fractions and $T$ is the total treatment time. Some other scholars (Maciejewski *et al.*, 1989; Thames *et al.*, 1990; Withers *et al.*, 1988; Yaes, 1989) also studied regrowth and regrowth delay in the LQ models. Therefore, by using this exponent in the LQ model, we have an LQ model as a function of dose and time,

$$S(D,t) = \mathrm{e}^{-\alpha D - \beta D^2/n}\, \mathrm{e}^{(ln(2)/T_d)(t-t_k)}, \tag{2.4}$$

where $T_d = \ln(2)/b$ is the tumour doubling time and $t_k$ is a time delay between the beginning of treatment and measurable regrowth of the tumour.

In brachytherapy (continuous radiation over time), the model is modified by using the Lea–Catcheside factor $G(t)$ (Kellerer & Rossi, 1972)

$$S(D) = \mathrm{e}^{-\alpha D - \beta G(t) D^2}. \tag{2.5}$$

The Lea−Catcheside factor describes the interaction of past radiation damage with current damage, where the interaction probability decays exponentially with rate $\gamma$ . The Lea−Catcheside factor is usually written for $t > T$ as

$$G(t) = \frac{2}{D(t)^2} \int_{-\infty}^{\infty} \dot{D}(\tau) \int_{-\infty}^{\tau} \mathrm{e}^{-\gamma(\tau - s)} \dot{D}(s)\, \mathrm{d}s\, \mathrm{d}\tau$$

or

$$G(T) = \frac{2}{D(T)^2} \int_{-\infty}^{T} \dot{D}(\tau) \int_{-\infty}^{\tau} \mathrm{e}^{-\gamma(\tau - s)} \dot{D}(s)\, \mathrm{d}s\, \mathrm{d}\tau,$$

where $\dot{D}(\tau)$ and $\dot{D}(s)$ are the dose rate, $D(t)$ is the cumulative dose and $T$ denotes the end of treatment. The Lea−Catcheside factor for endpoints $t > T$ has originally been derived from a lethal–potentially lethal model (LPL model) (Curtis, 1986). We can, however, use the same LPL model to derive a time-dependent Lea−Catcheside factor, which applies to all times $t > 0$. This formulation leads to our choice of $d_{\mathrm{eff}}(t)$ in (c) described subsequently. In that case, the Lea−Catcheside factor becomes:

$$G(t) = \frac{2}{D(t)^2} \int_{-\infty}^{t} \dot{D}(\tau) \int_{-\infty}^{\tau} \mathrm{e}^{-\gamma(\tau - s)} \dot{D}(s)\, \mathrm{d}s\, \mathrm{d}\tau. \tag{2.6}$$

Another approach, which is also based on clear physical principles, is the assumption of an effective interaction window for lesions (Dawson & Hillen, 2006). If two single hit events occur close in time, then there is a chance of an interaction. In this case, the survival fraction reads

$$S(D) = \exp\left(-\int_0^t [\alpha + 2\beta(D(s) - D(s-\omega))]\dot{D}(s)\mathrm{d}s\right),$$

where $\omega$ denotes the size of the effective interaction window.

### 2.2 *Hazard function*

We can use the concept of a hazard function to unify the above models into one formalism. The hazard function $h(t)$ describes the decay of survival fraction as

$$\frac{\mathrm{d}S(D(t))}{\mathrm{d}t} = -h(t)S(D(t)). \tag{2.7}$$

Zaider and Minerbo advertise the following hazard function for any form of treatment

$$h_1(t) := (\alpha + 2\beta D(t))\dot{D}(t) \tag{2.8}$$

If we solve (2.7) for the surviving fraction with hazard function $h_1(t)$ and initial condition $S(0) = 1$, we obtain

$$S(D(t)) = \exp\left(-\int_0^t h_1(s)\mathrm{d}s\right) = \exp(-\alpha D(t) - \beta D^2(t)). \tag{2.9}$$

*Case* 1: If we only give one treatment of dose $d$ and evaluate the above formula at the end of treatment $T$, then we get

$$S(D(T)) = \mathrm{e}^{-\alpha d - \beta d^2},$$

which is the LQ model (2.1).
*Case* 2: If, however, we give $n$ fractions of dose $d$, then at the end of treatment we obtain

$$S(D(T)) = \exp(-\alpha n d - \beta (nd)^2) \tag{2.10}$$

which does not correspond to the fractionated LQ formula (2.2). In (2.10), the $\beta$-term is overamplified by an additional factor of $n$, which, as we argue, leads to over-optimistic estimates for the TCP.

Based on (2.8) we rather propose the following form of hazard function for fractionated treatment:

$$h_2(t) := (\alpha + \beta d)\dot{D}(t). \tag{2.11}$$

The term $\beta d \dot{D}(t)$ describes the interaction of previous lesions with current radiation, which is on a small timescale compared to the treatment time $T$. If we solve (2.7) using $h_2(t)$, we obtain

$$S(D(t)) = \exp\left(-(\alpha + \beta d)D(t)\right),$$

which is exactly the LQ model (2.2).

More generality, we propose an effective interaction dose $d_{\mathrm{eff}}$, which includes the Lea−Catcheside factor, the fractionated schemes from above and the interaction window approach into one framework:

$$h_3(t) := (\alpha + \beta d_{\mathrm{eff}}(t))\dot{D}(t), \tag{2.12}$$

where

(a) $d_{\mathrm{eff}} = d$ for fractionated treatments,
(b) $d_{\mathrm{eff}}(t) = 2D(t)$ as in Zaider–Minerbo's formula (2.9) ,
(c) $d_{\mathrm{eff}}(t) = 2\int_{-\infty}^{t} \mathrm{e}^{-\gamma(t-s)}\dot{D}(s)\mathrm{d}s$ for the Lea−Catcheside factor and
(d) $d_{\mathrm{eff}}(t) = 2(D(t) - D(t-\omega))$ for the finite interaction window.

The corresponding survival fractions are

$$S(D(t)) = \exp\left(-\alpha D(t) - \beta \int_0^t d_{\text{eff}}(s)\dot{D}(s)\mathrm{d}s\right)$$

Especially,

(a)

$$S_a(D(t)) = \exp\left(-(\alpha + \beta d)D(t)\right) \tag{2.13}$$

(b)

$$S_b(D(t)) = \exp(-\alpha D(t) - \beta D^2(t)) \tag{2.14}$$

(c)

$$S_c(D(t)) = \exp(-\alpha D(t) - \beta G(t) D(t)^2), \text{ with } G(t) \text{ from (2.6)} \tag{2.15}$$

(d)

$$S_d(D(t)) = \exp\left(-\alpha D(t) - \beta \int_0^t 2(D(s) - D(s-\omega))\dot{D}(s)\mathrm{d}s\right). \tag{2.16}$$

There are several interesting special cases:
*Case* 1: If we consider fractionated treatment, and the interval $\omega$ includes one fractionation, then we can compute the integral in case (d) and find $S_d(t) = S_a(t)$ which is in agreement with the LQ model.
*Case* 2: If $\gamma \to 0$ in (c), then $d_{\text{eff}}(t) = 2D(t)$ and we obtain the Zaider–Minerbo formula (b). This shows that the approach (b) is useful if early lesions are not repaired and are always able to interact.
*Case* 3: If the interaction window in (d) is large ($\omega \to \infty$), we use the fact that $D(-\infty) = 0$ to see that (d) corresponds to (b). Hence, we get the same picture as in Case 2 above; model (b) implicitly assumes that interactions of radiation-induced lesions are on a long timescale.
*Case* 4: If the interaction window is small ($\omega \to 0$), then we redefine: $\tilde{\beta} = 2\beta\omega$ and we obtain

$$h_3(t) \; in \; (d) \to (\alpha + \tilde{\beta}\dot{D}(t))\dot{D}(t).$$

In this scenario, interactions would be strictly local in time.

In what follows, we will compare these different forms of hazard functions for the six models mentioned above. We find that the results for (c) Lea−Catcheside and (d) finite interaction window are virtually identical, while case (b) gives over-optimistic results.

### 2.3 *Poissonian TCP*

The simplest TCP models are based on the Poisson or the binomial distribution and the LQ survival fraction model. They both assume that the initial number of tumour cells $N_0$ is large. Let $X$ denote a random variable for the amount of surviving cells. If the death of tumour cells is stochastically independent of each other, and cell survival is a rare event, then we can assume $X$ is given by the Poisson distribution. The probability of $k$ tumour cells surviving is then,

$$p(X = k) = \frac{\lambda^k \, \mathrm{e}^{-\lambda}}{k!}. \tag{2.17}$$

Since the expectation of this distribution is $E(X) = \lambda$, we use the number of surviving cells $N_0 S(D)$ as an estimator for $\lambda$. Therefore, we have the Poisson TCP as

$$\mathrm{TCP_P} = p(X = 0) = \mathrm{e}^{-\lambda} = \mathrm{e}^{-N_0 S(D)}. \tag{2.18}$$

Similarly, the binomial TCP has the form

$$\mathrm{TCP_B} = (1 - S(D))^{N_0} \tag{2.19}$$

if the number of surviving cells $X$ satisfies a binomial distribution. The Poisson approximation tells us that the binomial distribution approaches the Poisson distribution when $N_0 \to \infty$, $S(D) \to 0$ and the product of $N_0 S(D)$ approaches the constant $\lambda$ (i.e. $N_0 S(D) \to \lambda$).

The survival fraction (2.4) includes linear regrowth. The corresponding ordinary differential equation (ODE) for linear regrowth is given by

$$\frac{\mathrm{d}N}{\mathrm{d}t} = (b - d)N(t) - h(t)N(t), \tag{2.20}$$

where $b$ denotes the mitosis rate and $d$ the natural death rate. We estimate the parameter $\lambda$ in the Poisson distribution (2.18) as the expected number of surviving tumour cells and obtain the one-compartment Poissonian TCP

$$\mathrm{TCP_{P_1}}(t) = \mathrm{e}^{-N(t)}. \tag{2.21}$$

In Gong *et al.* (2011), we also derived an explicit formula for non-linear regrowth. In order to compare with ZM TCP, where linear regrowth is used, we focus here on linear regrowth.

The two-compartment Poisson TCP can be calculated by the following system of ODEs for active ($a$) and quiescent cells ($q$) (Hillen *et al.*, 2010),

$$\frac{\mathrm{d}a}{\mathrm{d}t} = -\mu a + \nu q - (d_a + h_a(t))a, \tag{2.22}$$

$$\frac{\mathrm{d}q}{\mathrm{d}t} = 2\mu a - \nu q - (d_q + h_q(t))q. \tag{2.23}$$

Here, $h_a$ and $h_q$ are the hazard functions for active and quiescent cells and $d_a$ and $d_q$ are the natural death rates, respectively. The term $\mu$ gives the regrowth rate of active cells, and $\nu$ gives the switch rate of quiescent cells to active cells. We solve it numerically, and then evaluate

$$\mathrm{TCP_{P_2}}(t) = \mathrm{e}^{-(a(t)+q(t))}. \tag{2.24}$$

The two-compartment model in (2.22) and (2.23) is based on a more general two-compartment model in Hillen *et al.* (2010). The model in Hillen *et al.* (2010) allows cells after mitosis to become quiescent, or to continue in the cell cycle. Two special cases lead to the one-compartment model (2.20) on the one hand and the two-compartment model (2.22 and 2.23) on the other hand. In this paper, we focus on these two extreme cases. For a full discussion of the two-compartment models we refer to the literature (Dawson & Hillen, 2006; Hillen *et al.*, 2010).

### 2.4 *TCP based on birth–death processes*

When the number of tumour cells are small, stochastic effects dominate. In this case, deterministic models seem to be inappropriate for predicting the number of surviving cells. To accommodate the stochastic effects, Zaider & Minerbo (2000) employed a stochastic birth–death process. That is, the probability $P_i$ of $i$ tumour cells surviving at time $t$ is given by the master equation

$$\frac{\mathrm{d}P_i(t)}{\mathrm{d}t} = (i-1)bP_{i-1}(t) - i(b+d+h(t))P_i(t) + (i+1)(d+h(t))P_{i+1}(t), \quad i = 0, 1, 2, 3, \ldots \tag{2.25}$$

with the convention that $P_{-1} = 0$. The expected number of tumour cells $N(t) = \sum i P_i(t)$ satisfies the mean-field equation (2.20).

The mean-field description (2.20) of tumour cell proliferation and its death due to radiation is a reasonable approach when the number of cells is large. However, for a relatively small cell population (e.g. at the end of the treatment), the average behaviour is no longer adequate as probabilistic or stochastic noise becomes dominant.

By introducing a generating function, Zaider & Minerbo solved the master equation (2.25) and obtained an explicit expression for the TCP,

$$\mathrm{TCP}_{\mathrm{ZM}}(t) = P_0(t) = \left[1 - \frac{S_h(t)\,\mathrm{e}^{bt}}{1 + bS_h(t)\mathrm{e}^{bt}\displaystyle\int_0^t \frac{\mathrm{d}r}{S_h(t)\mathrm{e}^{bt}}}\right]^{N_0}. \tag{2.26}$$

Here

$$S_h(t) = \exp\left(-\int_0^t d + h(r)\,\mathrm{d}r\right) \tag{2.27}$$

is the probability of cell survival for a given hazard function $h(t)$ and natural death rate $d$. Dawson & Hillen (2006) simplified the Zaider–Minerbo TCP into

$$\mathrm{TCP}_{\mathrm{ZM}}(t) = \left[1 - \frac{N(t)}{N_0 + bN_0N(t)\displaystyle\int_0^t \frac{\mathrm{d}r}{N(r)}}\right]^{N_0}, \tag{2.28}$$

where $N$ solves the mean-field equation (2.20). Note that when $b = 0$, the Zaider–Minerbo TCP reduces to the binomial TCP.

In the previous section, we discussed the use of a two-compartment model to describe cell cycle effects. This extension can also be done for the birth–death process of Zaider and Minerbo (see Dawson & Hillen, 2006; Hillen *et al.*, 2010; O'Rourke *et al.*, 2009). The basic idea is the same as above, i.e. a detailed master equation for two compartments is used as a starting point. The mean-field equations are given by (2.22) and ( 2.23) and the TCP can again be expressed by the corresponding solutions of the mean-field equations. The resulting $\mathrm{TCP}_{\mathrm{DH}}$ formula is very complex and we refer to the original papers for reference (Dawson & Hillen, 2006; Hillen *et al.*, 2010).

### 2.5 *Monte Carlo method*

Another class of models for tumour growth are individual-based models (e.g. Hatzikirou & Deutsch, 2009; Kempf *et al.*, 2010). Here we use the Monte Carlo method as representative for this class of

models. The Monte Carlo method allows us to explicitly model the stochastic nature of cell–radiation interaction, cell proliferation and cell death. For the Monte Carlo simulations, we use the same birth and death probabilities as used in the master equation approach (2.25). The probability distributions for the random sampling in each time interval $\Delta t$ is given by:

- $b\Delta t$ for the probability of regrowth in a time interval of length $\Delta t$, where $b$ is the cell growth rate;
- $(d+h(t))\Delta t$ for probability of death in a time interval of length $\Delta t$, where $h(t)$ is the hazard function (2.12);
- $1-(d+b+h(t))\Delta t$ is the probability the cell remains unchanged in a time interval of length $\Delta t$.

For each simulation run and for each time-step, we define the treatment success indicator (TS($t$)) as:

$$\mathrm{TS}(t) = \begin{cases} 1, & \text{if } N(t) = 0, \\ 0, & \text{else,} \end{cases}$$

where $N(t)$ is the number of tumour cells at time $t$. TCP is therefore defined as the average of $M$ such independent simulations and is given by

$$\mathrm{TCP}(t) = \frac{1}{M}\sum_{i=1}^{M} \mathrm{TS}_i(t). \tag{2.29}$$

According to the law of large numbers, the error after $M$ samplings is the order of $1/\sqrt{M}$. In order to keep this error at an acceptable level, we simulate each case 300 times and the outcome is averaged. The output of the TCP curve as a function of time is relatively smooth, with a small standard deviation ($\approx 0.05$).

For the two-compartment models, we have two subpopulations governed by their own probability distributions according to Table 2:

- $\mu\Delta t$ for the probability of regrowth in a time interval of length $\Delta t$, where $\mu$ is the cell growth rate;
- $(d_a + h_a(t))\Delta t$ and $(d_q + h_q(t))\Delta t$ for probability of death in a time interval of length $\Delta t$ for the active and the quiescent cells, respectively, and $h_a(t)$, $h_q(t)$ are their hazard functions;
- $\nu\Delta t$ for the transition probability from quiescent into active cells in a time interval of length $\Delta t$;
- $1-(\mu + d_a + h_a(t))\Delta t$ and $1-(\nu + d_q + h_q(t))\Delta t$ are the probabilities that the cells remain unchanged in a time interval of length $\Delta t$ for the active and the quiescent cells, respectively.

The main drawback of the Monte Carlo method lies in its random nature: all the results are affected by statistical uncertainties which can be reduced at the expense of increasing the sample population and, hence, the computation time. This method is very convenient when the system has several degrees of freedom such as fluids (Prausnitz & Tavares, 2004) and cellular structures (Franks *et al.*, 2001), or when inputs are very uncertain, such as risk in business (Mathews, 2009). More broadly, Monte Carlo simulations have been applied to species dynamics in ecology, spatial sciences and oil exploration (Gonzalez-Parra *et al.*, 2010; Popov & Prokhorov, 2007) .

## 3. Treatment protocols and parameter values

In this section, we use seven treatment protocols for prostate cancer from the literature to compare the six models described in the previous section. Among them, three are standard treatments (labeled as

TABLE 1 *Seven treatment schedules for prostate cancer. A, C and D are standard treatments and e and f are two hyperfractionated treatments, where f is a high-dose brachytherapy.* $^{103}Pd$ *and* $^{125}I$ *are two permanent seeds brachytherapy treatments. Note that the brachytherapy treatments have no end time, since the radioactive seeds remain in the body. The column 'Total days' indicates the time when the total treatment dose is reached*

| Protocol | Dose/fraction ($d$ Gy) | Days/ week | Total days | Times/ day | Total dose | Reference |
|---|---|---|---|---|---|---|
| A | 2 | 5 | 53 | once | 78 | Reuther *et al.* (2002) |
| C | 3 | 5 | 26 | once | 60 | Livesey *et al.* (2003) |
| D | 4.3 | 5 | 16 | once | 51.6 | Liao *et al.* (2010) |
| e | 1.2 | 5 | 44 | twice | 76.8 | Parsons *et al.* (1988) |
| f | 6 | 5 | 4.5 | twice | 54 | Yoshioka *et al.* (2006) |

| Protocol | Initial dose | Decay rate $\lambda$ | Total days | Half times | Total dose | Reference |
|---|---|---|---|---|---|---|
| $^{103}Pd$ | 5.71 | 0.0408 | 47.63 | 16.99 | 120 | Nag *et al.* (1999) |
| $^{125}I$ | 1.86 | 0.0117 | 207.8 | 59.4 | 145 | Nag *et al.* (1999) |

$A, C, D$). These are given once per day on weekdays with weekends off. The others are one hyperfractionated treatment (labeled as $e$), one high dose rate brachytherapy (labeled as $f$) and two permanent seeds brachytherapies ($^{103}Pd$, $^{125}I$) (see Table 1).

For computational simplicity, we assume that all radiation protocols start on a Monday. Fractionated treatments $A, C, D, e$ and $f$ are given on weekdays with weekends off. We assume it takes 10 min to deliver each fraction of the dose at a constant dose rate. If the protocols prescribe one fraction per day (called standard treatments), treatments are delivered at 12:00 pm (noon); in the case of two fractions per day (called hyperfractionated treatments), treatments are delivered at 12:00 and 6:00 pm.

To compare parameter values between one- and two-compartment models, we use weighted averages. In the two-compartment model (2.22) and (2.23), the transition rate from active to quiescent is $\mu$ and the transition rate for quiescent to active is $\nu$. Hence, assuming Poisson process for the transition events, the average time spent in the active phase is $1/\mu$ and in the quiescent phase $1/\nu$ (Thieme, 2003). The parameter values will be different for active and quiescent compartments, e.g. the $\beta$ value of the radiosensitivities. In general, let $p_{\text{one}}$ be a parameter in the one-compartment model and $p_a$, $p_q$ parameters for active and quiescent cells, respectively. Then the parameters are related by the following equation

$$p_{\text{one}} = p_a \frac{1/\mu}{1/\mu + 1/\nu} + p_q \frac{1/\nu}{1/\mu + 1/\nu}. \tag{3.1}$$

The parameters used in the two-compartment model are listed in the $\text{TCP}_{\text{DH}}$ column in Table 2, and the parameters for the one-compartment model are in column $\text{TCP}_{\text{ZM}}$. In most publications on cancer growth, the effective net growth rate is reported. We use these values to estimate the net growth rate $b-d$. The parameters of the one-compartment models are related to the parameters of the two-compartment model via the weighted averaging described above (3.1). We will see later that this is indeed a good choice as the models behave quite similarly.

The permanent seeds have dose rate $\dot{D}(t) = R_0 \, \mathrm{e}^{-\lambda t}$, which is a continuous function of time $t$. In the case of fractionated treatments (protocols $A, C, D, e$ and $f$ from Table 1), $\dot{D}(t)$ are jump functions. Because of the differences in the dose rates of these treatments, we report their results separately.

TABLE 2 *Table of parameters and references. Column* $\mathrm{TCP_{DH}}$ *refers to the two-compartment model,* $\mu$ *is the birth rate of its active tumour cells and* $\nu$ *is the transition rate from quiescent into active cells.* $\alpha_a, \beta_a, \alpha_q$ *and* $\beta_q$ *are radiosensitive parameters of the LQ model for active and quiescent cells, respectively. Column* $\mathrm{TCP_{ZM}}$ *refers to the parameters for one-compartment models, which are calculated by (3.1) based on the values in column* $\mathrm{TCP_{DH}}$. *Besides the initial tumour size* $10^6$, *we also simulate for* $N(0) = 10^2, 10^4, 10^5, 10^{10}$, which give similar results; hence, we choose to only present the results for $10^6$

| | $\mathrm{TCP_{ZM}}$ | $\mathrm{TCP_{DH}}$ | Unit | Reference |
|---|---|---|---|---|
| Initial cell | $N(0) = 10^6$ | $a(0) + q(0) = 10^6$ | cells | Strigari *et al.* (2008) |
| Net growth rate | $b - d = 0.0273$ | $\mu - d_a = 0.0655$ | 1/day | Swanson *et al.* (2001) |
| | | $\nu - d_q = 0.0476$ | 1/day | Basse *et al.* (2002) |
| $\alpha$ | $\alpha = 0.1531$ | $\alpha_a = 0.145$ | $\mathrm{Gy^{-1}}$ | Carlson *et al.* (2004) |
| | | $\alpha_q = 0.159$ | $\mathrm{Gy^{-1}}$ | Carlson *et al.* (2004) |
| $\beta$ | $2\beta = 2 \times 0.0149$ | $2\beta_a = 0.070646$ | $\mathrm{Gy^{-2}}$ | Carlson *et al.* (2004) |
| | | $2\beta_q = 0$ | | Assumption |

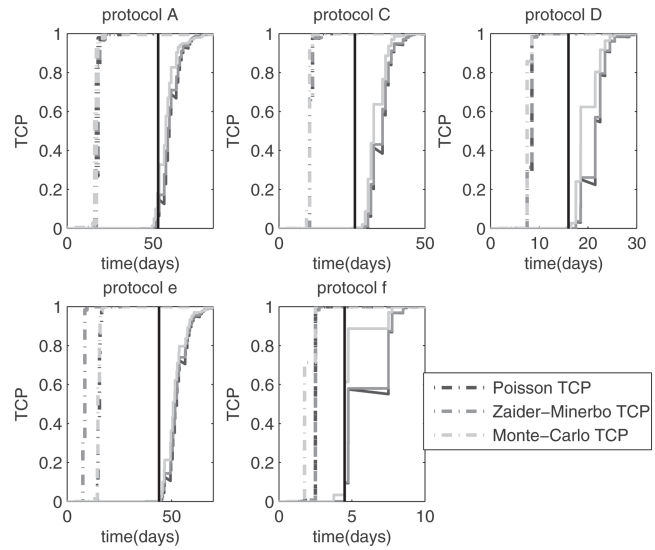


FIG. 1. TCP for treatment $A, C, D$ and $e, f$ as function of time, with survival fraction (2.14) (and corresponding hazard function (2.8)) and survival fraction (2.13) (or equivalently (2.16)). Each subplot shows two groups of three curves. The left groups correspond to (2.14) while the right group corresponds to (2.13). The vertical line on each subplot is the treatment ending time. Blue lines are for Poissonian TCP (1-P), cyan lines for Zaider–Minerbo (ZM) TCP (1-ZM) and red for Monte Carlo TCP (1-MC). All the parameter values are from Table 2.

## 4. Results

### 4.1 *Fractionated treatments*

In Fig. 1 we show the time course of the TCP for the three one-compartment models (1-P), (1-ZM) and (1-MC). The five subplots refer to the five fractionated treatments $A, C, D, e$ and $f$, where the vertical line indicates the end time of these treatments. Within each figure we show two groups of

three curves. The left group of three curves corresponds to the survival fraction described by (2.14), whereas the right group of curves corresponds to the survival fraction for fractionated treatments (2.13). Instead of using (2.13) directly, we use (2.16), which is equivalent to (2.13) for fractionated treatment, as mentioned earlier. This choice allows us later to use the same formulation for brachytherapy as well as for any other time-dependent treatment method. In Li *et al.* (2003), the best estimate of the average tumour DNA repair time is 16 min. That is to say, one DNA damage can only interact with another to create a double-strand break, if they occur within 16 min.. Hence, we choose an interaction window of $\omega = 16$ min, such that any dose delivered to a patient within this window will count towards the hazard function, as Dawson & Hillen (2006) proposed.

The simulations clearly show that the three models make the same predictions. The hazard function (2.8) shows clearly over-optimistic results, while the results using the effective interaction dose $d_{\text{eff}}$ are more plausible. The computation of absolute TCP values is not the point of this paper. The point is to show that these three very different methods show virtually identical TCP predictions. Hence, they are equally useful for treatment outcome predictions.

In Fig. 2 we plot the TCPs as a function of dose. Again, we see that the curves that correspond to the same choice of $h(t)$ are very close. The numbers in each subplot are the $D_{50}$ value for the Poissonian TCP. We do not show the $D_{50}$ values for the other models, since they are very close as we can see from the graph. We compared our $D_{50}$ values with those reported by Levegrun *et al.* (2002) from clinical data for prostate cancer. Our values for $C$, $D$ and $f$ are all in the 95% confidence intervals of their $D_{50}$ values. Our $D_{50}$ values for $A$, $e$ are a bit higher than the values reported by Levegrun *et al.* (2002).

We also compare the three one-compartment models with their two-compartment models by using the parameters from Table 2. The results for protocols $C$ and $e$ are reported in Fig. 3. We find that the difference between the one-compartment and two-compartment models are negligible for hyperfractionated

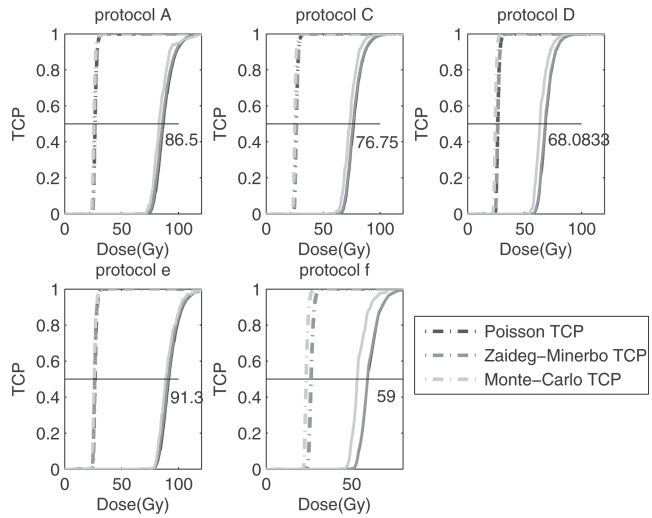


FIG. 2. TCP for treatment $A$, $C$, $D$ and $e$, $f$ as function of dose, with survival fraction (2.14) (and corresponding hazard function (2.8)) and survival fraction (2.13) (or equivalently (2.16)). Each subplot is the result for one treatment shown on the top. The lines gathering on the left part of each subplot are results by using hazard function (2.8), whereas ones on the right part are results calculated with (2.11). Horizontal line denotes the $D_{50}$ position where TCP $= 0.5$. Blue lines are for Poissonian TCP, cyan lines for ZM TCP and red for Monte Carlo TCP. All the parameter values are from Table 2.

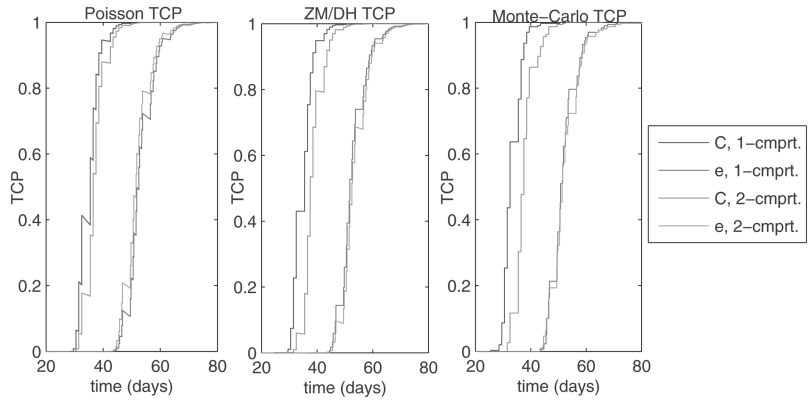


FIG. 3. TCP as a function of time, using protocols $C$ and $e$, for both the one- and two-compartment models. The left panel is for the Poisson TCPs ((1-P) and (2-P)), the middle panel is for the ZM and Dawson–Hillen TCPs ((1-ZM) and (2-DH), respectively) and the right panel is for the Monte Carlo TCPs ((1-MC) and (2-MC)). All parameters are taken from Table 2 and the effective dose hazard function (2.12)(d) is used.

treatment $e$, while for standard treatment schedules $C$ two-compartment TCPs are shifted to the right by at most 5 days. We have similar results for the other treatment protocols. Hence, the existence of a quiescent compartment allows clonogenic cells to be sequestered from radiation and to repopulate the tumour between treatments.

### 4.2 *Brachytherapy treatments*

A standard model for brachytherapy treatments is the hazard function with the Lea−Catcheside protraction factor (2.12)(c) and survival fraction (2.15). We will show that this choice of hazard function can be approximated by the effective interaction window hazard function (2.12)(d) and survival fraction (2.16). The Lea−Catcheside protraction factor is simple enough to program directly. However, by using the time-window approach, we will be able to find a hazard function which is equally applicable to fractionated therapies and to brachytherapy.

Choosing the total dose as for a radioactive seed as in (1.1), the Lea–Catcheside factor (2.6) can be explicitly computed as

$$G(t) = \frac{2R_0^2}{D(t)^2(\gamma - \lambda)}\left[\frac{1 - \mathrm{e}^{-2\lambda t}}{2\lambda} + \frac{\mathrm{e}^{-(\lambda+\gamma)t} - 1}{\lambda + \gamma}\right]. \tag{4.1}$$

Once again, $R_0$ is the initial dose rate, $D(t)$ is the total dose absorbed, $\lambda$ is the average half-life for the permanent seed and $\omega = \ln(2)/\gamma$ is the lifetime of the DNA double-strand breaks, which was chosen to be the same as in the effective dose, 16 min. In what follows, we show mathematically that the effective dose hazard function and Lea–Catcheside hazard function are almost the same, when both have the same parameters.

From (2.7) we can compute the Lea–Catcheside hazard function as

$$h_{\mathrm{LC}}(t) = \frac{dS_{\mathrm{LC}}(t)/\mathrm{d}t}{-S_{\mathrm{LC}}(t)} = \alpha \dot{D(t)} + \beta \frac{\mathrm{d}(\mathrm{G(t)D(t)^2})}{\mathrm{d}t} = \alpha R_0 \,\mathrm{e}^{-\lambda t} + \beta \frac{2R_0^2}{\gamma - \lambda}(\mathrm{e}^{-2\lambda t} - \mathrm{e}^{-(\lambda+\gamma)t}), \tag{4.2}$$

where we use (4.1) in the last equality.

By using the formula (1.1) in (2.12)(d), we have an effective dose hazard function as follows:

$$h_{\text{eff}}(t) = \alpha R_0 \, \mathrm{e}^{-\lambda t} + 2\beta \frac{R_0^2}{\lambda}(\mathrm{e}^{-2\lambda t+\lambda\omega} - \mathrm{e}^{-2\lambda t}). \tag{4.3}$$

The difference between $h_{\text{eff}}(t)$ and $h_{\text{LC}}(t)$ is

$$\begin{aligned}
\frac{h_{\text{eff}}(t) - h_{\text{LC}}(t)}{2\beta R_0^2} &= \frac{\mathrm{e}^{-2\lambda t+\lambda\omega} - \mathrm{e}^{-2\lambda t}}{\lambda} - \frac{\mathrm{e}^{-2\lambda t} - \mathrm{e}^{-(\gamma+\lambda)t}}{\gamma - \lambda} \\
&= \frac{\mathrm{e}^{-2\lambda t+\lambda\omega}(\gamma - \lambda) - \mathrm{e}^{-2\lambda t}(\gamma - \lambda) - \lambda \mathrm{e}^{-2\lambda t} + \lambda \mathrm{e}^{-(\gamma+\lambda)t}}{\lambda(\gamma - \lambda)} \\
&= \frac{\mathrm{e}^{-2\lambda t+\lambda\omega}(\gamma - \lambda) - \gamma \, \mathrm{e}^{-2\lambda t}}{\lambda(\gamma - \lambda)} + \frac{\mathrm{e}^{-(\gamma+\lambda)t}}{\gamma - \lambda} \\
&= \mathrm{e}^{-2\lambda t}\left[\frac{\mathrm{e}^{\lambda\omega}}{\lambda} - \frac{\gamma}{\lambda(\gamma - \lambda)}\right] + \frac{\mathrm{e}^{-(\gamma+\lambda)t}}{\gamma - \lambda}.
\end{aligned}$$

Because $\gamma = ln(2)/\omega = 62.38 \gg \lambda$, we have the following estimate

$$|h_{\text{eff}} - h_{\text{LC}}| \leqslant 2\beta R_0^2 \left| \mathrm{e}^{-2\lambda t}\left(\frac{\mathrm{e}^{\lambda\omega}}{\lambda} - \frac{1}{\lambda}\right) + \frac{\mathrm{e}^{-(\gamma+\lambda)t}}{\gamma - \lambda} \right| \leqslant 2\beta R_0^2 \left| \frac{\mathrm{e}^{\lambda\omega}}{\lambda} - \frac{1}{\lambda} + \frac{1}{\gamma - \lambda} \right|. \tag{4.4}$$

The last expression equals 0.0626 for $^{103}Pd$ and 0.0066 for $^{125}I$, when using the parameters in Table 2. Hence, the difference between these two approaches is very small. We show numerical simulations of our three one-compartment models for these two types of hazard functions in Fig. 4 and we find them to be indistinguishable. Also, if we compare the TCP for the three models (1-P), (1-ZM) and (1-MC), they are also virtually identical, hence, they give the same predictions.

Note that the $^{103}Pd$ curves for the Poissonian model do start to decay after about 110 days. The Poisson TCP formula is based on the mean-field differential equations and, consequently, the number of tumour cells can never be identical to zero. Hence after radiation subsides, the tumour will always regrow. The other two models (1-ZM) and (1-MC) have the advantage that the tumour can be eradicated in finite time and it does not recur. Hence, the decline in TCP after treatment is an artifact of the Poissonian model.

### 4.3 *Dependence of growth rate b and survival fraction $S(d)$*

In order to investigate how the models depend on the tumour growth rate and the radiosensitivity of the tumour, we compute the TCP for different effective growth rates $b$ and survival fractions $S(d)$. For matters of space, we show only protocol $C$. The behaviour is very similar for the other protocols.

We study the TCP dependence on the growth rate in Fig. 5: In (a) we plot the pairwise distance of the TCP curves between the three one-compartment models as a function of the growth rate in a semilogarithmic plot. We measure the distance in the $L^2$-norm, which corresponds to the squared error sum. We see that the distance between Zaider–Minerbo TCP and Poissonian TCP is always smaller

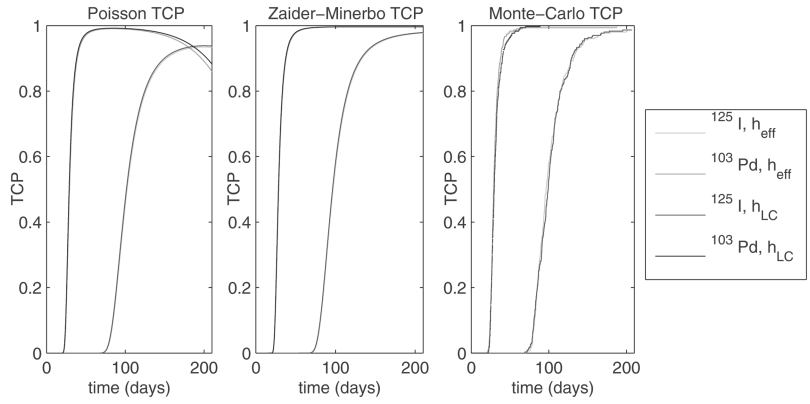


FIG. 4. TCP as a function of time for permanent seed treatment with $^{103}Pd$ and $^{125}I$, with the effective dose hazard function (4.3) and the Lea–Catcheside hazard function (4.2). The left panel is for the Poissonian TCP, the middle panel is for the ZM TCP and the right panel is for the Monte Carlo TCP. Parameter values are from Table 2.

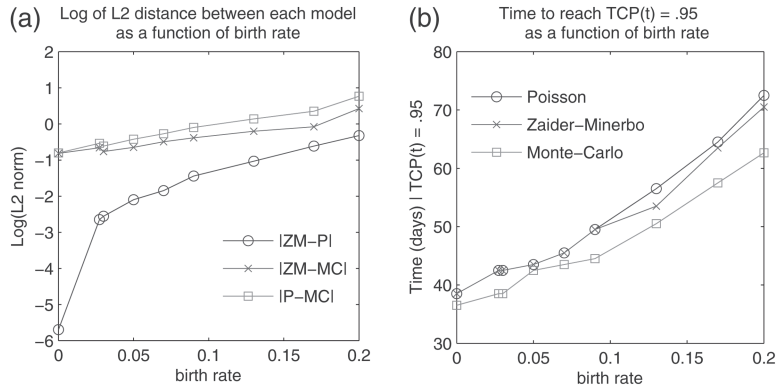


FIG. 5. (a) Semilogarithmic plot of the pairwise $L^2$-distance between the TCP curves as a function of the birth rate $b$, for treatment protocol $C$. (b) Time at which the TCP curve reaches 95% as a function of the birth rate $b$. We use effective dose hazard function (2.12)(d) here and all parameters except the birth rate are taken from Table 2.

than $e^{-2} = 0.14$ when the regrowth rates are in the interval of [0, 0.07], but the distance increases with increasing $b$; however, it is still very small over all ($<e^{-1}$). The Monte Carlo TCP shows a bigger distance to the other two, but still smaller than $e^1$ even for the highest growth rate.

In Fig. 5(b) we record the time when the TCP values reach 95% success. Again the model predictions are very close, with a slight increased difference for large birth rate values.

Now changing the survival fraction by varying the radiosensitivity parameter $\beta$, we plot the graphs in Fig. 6. We show the log-$L^2$ distance in Fig. 6(a) as a function of survival fraction $S(d)$. Figure 6(b) shows the time at which TCP = 95% as a function of $S(d)$. We see from (b) that the time reaching 95% TCP sensitively depends on $S(d)$ but the three models behave the same.

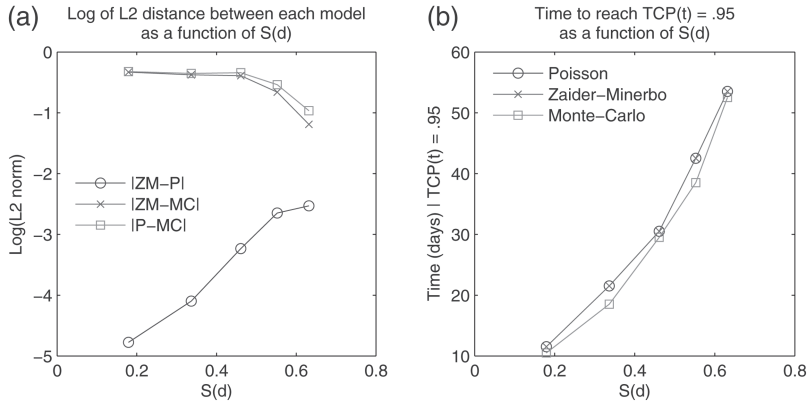


FIG. 6. (a) Semilogarithmic plot of the pairwise $L^2$-distance between the TCP curves for treatment protocol $C$ as function of the survival fraction $S(d)$. (b) Time at which the TCP curve reaches 95% as a function of the survival fraction $S(d)$. $S(d)$ is varied by changing $\beta$ and all other parameters are taken from Table 2; effective dose hazard function (2.12)(d) is used.

## 5. Conclusions

We initiated this line of research since we expected, based on experience, that the more complicated models indeed make the same predictions as the simplest model, the Poissonian TCP. Through our systematic study we can confirm this observation. We simulated many more parameter values as presented here and the discrepancy between Poisson models, birth–death models and Monte Carlo simulations is always small. During our studies we found in the literature that the relation between survival fraction and hazard function is often unclear and not well presented. Hence, we tried to summarize and compare the different forms of $h$ and $S(D)$ which are discussed in the literature. Different hazard functions are used for fractionated therapies as opposed to brachytherapies. As a side result, we found that using the effective interaction window in (2.12)(d), we were able to unify these two approaches into one framework. We showed that (2.12)(d) can equally be applied to fractionated therapies as well as brachytherapies. As for fractionated treatments, it corresponds to the standard fractionated survival fraction and for brachytherapy it corresponds to the Lea−Catcheside factor.

The Poisson TCP is simple and computationally efficient. We simulated the three models on the same computer: Intel Core 2 Duo, 2.0GHz and 2GB DDR2. For one typical simulation the Poisson TCP takes 3.34 s, the Zaider–Minerbo TCP uses 65.4 s and the Monte Carlo TCP uses up to 2.3 h. Therefore, for slow-proliferating tumours, we suggest that the Poisson TCP be used for calculations. However, when birth rate increases, the difference between Poisson TCP and Zaider–Minerbo TCP increases. For example in Fig. 5, the difference between Poisson and Zaider–Minerbo TCP enlarges to 2 days when the growth rate is 0.2. This confirms the results of Tucker *et al.* (1990), who showed that the Poisson TCP can underestimate the tumour cure up to 15% when the tumour doubling time is 2.06 days (or growth rate 0.34), which is a very fast growing tumour. Furthermore, the change of the survival fraction parameter $\beta$ will also slightly magnify the difference between the three TCP models.

As for the low dose rate brachytherapy, the Poisson TCP is much more sensitive to the number of tumour cells. After the end of treatment, the growth of tumour cells (therefore the increase of tumour cell numbers) causes the Poisson TCP to decrease. On the other hand, the Zaider–Minerbo and Monte Carlo TCP remain constant. This is a clear advantage of the stochastic models of Zaider–Minerbo and Monte Carlo. As soon as all cells are eradicated the tumour is gone forever. The Poissonian TCP, however, is

based on an ODE formulation. Here solutions only converge to zero but will never reach zero in finite time. Hence, in the Poissonian formulation a tumour will always recur.

We also compare Poisson, Zaider–Minerbo and Monte Carlo TCP with their corresponding two-compartment TCP models, where the cell cycle effect is included through a quiescent compartment. While the result between the two-compartment models are the same, there is a significant difference between one- and two-compartment models. The two-compartment models give less optimistic predictions and they suggest longer treatment periods. This is related to the fact that quiescent cells are less sensitive to radiation and they can be reactivated by the death of the surrounding active cells. Nutrients become available to the quiescent cells and they enter the cell cycle and repopulate the tumour. Hence, it is critical to control the most radioresistant cells.

In this paper, we use prostate cancer treatments as test cases for our simulations. We expect, however, that similar conclusions hold true for other localized tumours such as those in pancreas, colon, liver, etc.

Overall, the differences in all the models which we study are small. We have to evaluate this within the treatment of a real tumour. There are many important aspects which we do not include in our models, such as immune response, spatial structure of the tumour, vascularization, metastasis, genetic instabilities and relevant biochemical pathways. Compared to all these details, which are still missing from the models, the TCP models considered here are basically identical. Our study confirms the usefulness of the Poissonian formulation and we feel that more complicated models should only be used when absolutely necessary.

## Acknowledgements

We are extremely grateful for a number of highly constructive remarks from Leonid Hanin (Idaho State University), which helped to improve this paper.

## Funding

Natural Sciences and Engineering Research Council (NSERC) of Canada (8532227); Emerging Leaders in the Americas Program (ELAP).

## References

American Cancer Society. Available at http://www.cancer.org/docroot/home/index.asp.

Basse, B., Baguley, B. C., Marshall, E. S., Joseph, W. R., van Brunt, B., Wake, G. & Wall, D. J. N. (2002) A mathematical model for analysis of the cell cycle in human tumour. *J. Math. Biol.*, **47**, 295–312.

Cancer Facts and Figures. (2011) Available at http://www.cancer.org/acs/groups/content/@epidemiology surveilance/documents/document/acspc-029771.pdf.

Carlson, D. J., Stewart, R. D., Li, X. A., Jennings, K., Wang, J. Z. & Guerrero, M. (2004) Comparison of *in vitro* and *in vivo* $\alpha/\beta$ ratios for prostate cancer. *Phys. Med. Biol.*, **49**, 4477–4491.

Curtis, S. B. (1986) Lethal and potentially lethal lesions induced by radiation—a unified repair model. *Radiat. Res.*, **106**, 252–271.

Dawson, A. & Hillen, T. (2006) Derivation of the tumour control prabability (TCP) from a cell cycle model. *Comput. Math. Methods Med.*, **7**, 121–142.

Fowler, J. F. (1989) The linear-quadratic formula and progress in fractionated radiotherapy. *Br. J. Radiol.*, **62**, 679–694.

Franks, K. M., Bartol, T. M. & Sejnowski, T. J. (2001) An M-cell model of calcium dynamics and frequency-dependence of calmodulin activation in dendritic spines. *Neurocomputing*, **38**, 9–16.

GONG, J. & HILLEN, T. (2011) Optimal cancer radiotherapy treatment schedules under cumulative radiation effect constraint. *Math. Biosci.* (submitted).

GONZALEZ-PARRA, G., ARENAS, A. J. & SANTONJA, F. J. (2010) Stochastic modeling with Monte Carlo of obesity population. *J. Biol. Syst.*, **18**, 93–108.

HANIN, L. G. (2001) Iterated birth and death process as a model of radiation cell survival. *Math. Biosci.*, **169**, 89–107.

HANIN, L. G. (2004) A stochastic model of tumor response to fractionated radiation: limit theorems and rate of convergence. *Math. Biosci.*, **91**, 1–17.

HANIN, L. G., ZAIDER, M. & YAKOVLEV, A. Y. (2001) Distribution of the number of clonogens surviving fractionated radiotherapy: a long-standing problem revisited. *Int. J. Radiat. Biol.*, **77**, 205–213.

HATZIKIROU, H. & DEUTSCH, A. (2009) Cellular automata models of tumor invasion. *Encyclopedia of Complexity and Systems Science*, pp. 919–922.

HILLEN, T., DE VRIES, G., GONG, J. & FINLAY, C. (2010) From cell population models to tumour control probability: including cell cycle effects. *Acta Oncol.*, **7**, 121–142.

HORAS, J. A., OLGUIN, O. R. & RIZZOTTO, M. G. (2010) Examining the validity of Poissonian models against the birth and death TCP models for various radiotherapy fractionation schemes. *Int. J. Radiat. Biol.*, **86**, 711–717.

KAANDERS, J. H. A. M., POP, L. A. M., MARRES, H. A. M., BRUASET, I., VAN DEN HOOGEN, F. J. A., MERKX, M. A. W. & VAN DER KOGEL, A. J. (2002) Arcon: experience in 215 patients with advanced head-and-neck cancer. *Int. J. Radiat. Oncol. Biol. Phys.*, **52**, 769–778.

KELLERER, A. M. & ROSSI, H. H. (1972) The theory of dual radiation action. *Curr. Top. Radiat. Res. Q.*, **8**, 85–158.

KEMPF, H., BLEICHER, M. & MEYER-HERMANN, M. (2010) Spatio-temporal cell dynamics in tumour spheroid irradiation. *Eur. Phys. J. D*, **60**, 177–193.

LEVEGRUN, S., JACKSON, A., ZELEFSKY, M. J., VENKATRAMAN, E. S., SKWARCHUK, M. W., SCHLEGEL, W., FUKS, Z., LEIBEL, S. A. & LING, C. C. (2002) Risk group dependence of dose-response for biopsy outcome after three-dimensional conformal radiation therapy of prostate cancer. *Radiother. Oncol.*, **63**, 11–26.

LI, X. A., WANG, J. Z., STEWART, R. D. & DIBIASE, S. J. (2003) Dose escalation in permanent brachytherapy for prostate cancer: dosimetric and biological considerations. *Phys. Med. Biol.*, **48**, 2753–2765.

LIAO, Y., JOINER, M., HUANG, Y. & BURMEISTER, J. (2010) Hypofractionation: what does it mean for prostate cancer treatment? *Br. J. Radiol.*, **76**, 260–268.

LIVESEY, J. E., COWAN, R. A., WYLIE, J. P., SWINDELL R., READ G., KHOO V. S., LOGUE J. P. (2003) Hypofractioated conformalradio therapy in carcinoma of the prostate: five-year outcome analysis. *Int. J. Radiat. Oncol. Biol. Phys.*, **57**, 1254–1259.

MACIEJEWSKI, B., WITHERS, H. R., TAYLOR, J. M. G. & HLINIAK, A. (1989) Dose fractionation and regeneration in radiotherapy for cancer of the oral cavity and oropharynx—tumor dose-response and repopulation. *Int. J. Radiat. Oncol. Biol. Phys.*, **16**, 7831–7843.

MAH, K., VAN DYK, J. & POON, P. Y. (1987) Acute radiation induced pulmonary damage: a clinical study on the response to fractionated radiation therapy. *Int. J. Radiat. Oncol. Biol. Phys.*, **13**, 179–188.

MALER, A. & LUTSCHER, F. (2010) Cell cycle times and the tumor control probability. *Math. Med. Biol.*, **27**, 313–342.

MATHEWS, S. (2009) Valuing risky projects with real options. *Res. Technol. Manag.*, **52**, 32–41.

NAG, S., BEYER, D., FRIEDLAND, J., GRIMM, P. & NATH, R. (1999) American Brachytherapy Society (abs) recommendations for transperineal permanent brachytherapy of prostate cancer. *Int. J. Radiat. Oncol. Biol. Phys.*, **44**, 789–799.

O'ROURKE, F., MCANENEY, H. & HILLEN, T. (2009) Linear quadratic and tumour control probability modelling in external beam radiotherapy. *J. Math. Biol.*, **58**, 799–817.

PARSONS, J. T., MENDENHALL, W., CASSISI, N., ISASCS, J. & MILLION, R. R. (1988) Accelerated hyperfractionation for head and neck cancer. *Int. J. Radiat. Oncol. Biol. Phys.*, **14**, 649–658.

POPOV, S. B. & PROKHOROV, M. E. (2007) Population synthesis in astrophysics. *Phy. Usp.*, **50**, 1123–1146.

PRAUSNITZ, J. M. & TAVARES, F. W. (2004) Thermodynamics of fluid-phase equilibria for standard chemical engineering operations. *Aiche J.*, **50**, 739–761.

PROSTATE CANCER CANADA. Available at http://www.prostatecancer.ca/PCCN/Prostate-Cancer/Treatment/Brachytherapy.

REUTHER, A. M., WILLOUGHBY, T. R. & KUPELIAN, P. A. (2002) Toxicity after hypofractionated external beam radiotherapy (70 gy at 2.5 gy per fraction) versus standard fractionation radiotherapy (78 gy at 2.0 gy per fraction) for localized prostate cancer. *Int. J. Radiat. Oncol. Biol. Phys.*, **54** (Suppl. 1), 187–188.

STAVREVA, N. A., STAVREV, P. V., WARKENTIN, B. & FALLONE, B. G. (2003) Investigating the effect of cell repopulation on the tumor response to fractionated external radiotherapy. *Med. Phys.*, **30**, 735–742.

STRIGARI, L., D'ANDREA, M., ABATE, A. & BENASSI, M. (2008) A heterogeneous dose distribution in simultaneous integrated boost: the role of the clonogenic cell density on the tumor control probability. *Phys. Med. Biol.*, **53**, 5257–5273.

SWANSON, K. R., TRUE, L. D., LIN, D. W., BUHLER, K. R., VESSELLA, R. & MURRAY, J. D. (2001) A quantitative model for the dynamics of serum prostate-specific antigens as a marker for cancerous growth. *Am. J. Pathol.*, **158**, 2195–2199.

THAMES, H. D., BENTZEN, S. M., TURESSON, I., OVERGAARD, M. & VANDENBOGAERT, W. (1990) Time-dose factors in radiotherapy—a review of the human data. *Radiother. Oncol.*, **19**, 219–235.

THIEME, H. R. (2003) *Mathematics in Population Biology*. Princeton, NJ: Princeton University Press.

TRAVIS, E. L. & TUCKER, S. L. (1987) Isoeffect models and fractionated radiation-therapy. *Int. J. Radiat. Oncol. Biol. Phys.*, **13**, 283–287.

TUCKER, S. L., THAMES, H. D. & TAYLOR, J. M. G. (1990) How well is the probability of tumor cure after fractionated-irradiation described by Poisson statistics. *Radiat. Res.*, **124**, 273–282.

WHELDON, T. E. (1988) *Mathematical Models in Cancer Research*. Bristol, UK: Taylor and Francis.

WITHERS, H. R., TAYLOR, J. M. G. & MACIEJEWSKI, B. (1988) The hazard of accelerated tumor clonogen repopulation during radiotherapy. *Acta Oncol.*, **27**, 131–146.

WORLD HEALTH ORGANIZATION (2008). *World Cancer Report 2008*.

YAES, R. J. (1989) Linear-quadratic model isoeffect relations for proliferating tumor-cells for treatment with multiple fractions per day. *Int. J. Radiat. Oncol. Biol. Phys.*, **17**, 901–905.

YAKOVLEV, A. Y. (1993) Comments on the distribution of clonogens in irradiated tumors. *Radiat. Res.*, **134**, 117–120.

YOSHIOKA, Y., KONISHI, K., OH, R., SUMIDA, L., YAMAZAKI, H., NAKAMURA, S., NISHIMURA, K. & NONOMURA, N. (2006) High-dose-rate brachytherapy without external beam irradiation for locally advanced prostate cancer. *Radiother. Oncol.*, **80**, 62–68.

ZAIDER, M. & MINERBO, G. N. (2000) Tumour control probability: a formulation applicable to any temporal protocol of dose delivery. *Phys. Med. Biol.*, **45**, 279–293.